Phosphorus and nitrogen co-doped carbon derived from Cigarette Filter for adsorption of methylene blue dye from aqueous solution

Samantha Macchi
University of Arkansas at Little Rock https://orcid.org/0000-0002-7546-4200
Zane Alsebai
Little Rock Central High School
Fumiya Watanabe
University of Arkansas at Little Rock
Arooba Ilyas
University of Arkansas at Little Rock
Shiraz Atif
University of Arkansas at Little Rock
Tito Viswanathan
University of Arkansas at Little Rock
Noureen Siraj (nxsiraj@ualr.edu)
University of Arkansas at Little Rock https://orcid.org/0000-0003-4925-0265

Research

Keywords: doped carbon, adsorption, green chemistry, microwave, cigarette

Posted Date: May 14th, 2021

DOI: https://doi.org/10.21203/rs.3.rs-507326/v1

Phosphorus and nitrogen co-doped carbon derived from Cigarette Filter for adsorption of methylene blue dye from aqueous solution

Samantha Macchi[1], Zane Alsebai[2], Fumiya Watanabe[3], Arooba Ilyas[1], Shiraz Atif[1], Tito Viswanathan[1] and Noureen Siraj[1,*]

[1] Department of Chemistry, University of Arkansas at Little Rock, 2801 S. University Ave, Little Rock, AR 72204, USA

[2] Little Rock Central High School, 1500 Park Street, Little Rock, AR 72202, USA

[3] Center for Integrative Nanotechnology Sciences, University of Arkansas at Little Rock, 2801 S. University Ave, Little Rock, AR 72204, USA

* Correspondence: nxsiraj@ualr.edu

Abstract

Global access to sanitary water is of utmost importance to human health. Presently, textile dye water pollution and cigarette pollution are both plaguing the environment. Herein, waste cigarette filters are converted into useful carbon-based adsorbent materials via a facile, microwave-assisted carbonization procedure. The cigarette filters are co-doped with phosphorus and nitrogen using ammonium polyphosphate to enhance their surface characteristics and adsorbent capability. The adsorbents are characterized physically to examine their surface area, elemental composition, and surface charge properties. Batch adsorption experiments were performed to determine the maximum adsorption capacity of the adsorbents. Additionally, the effects of various adsorption parameters— temperature, adsorbent dosage, pH, and time—on adsorption process were examined. The doped adsorbent showed a maximum adsorption capacity of 303.3 mg g^{-1} respectively, which is three times that of the methylene blue adsorption capacity of commercially available activated carbon (~100 mg g^{-1}). Thus, the phosphorus and nitrogen co-doped carbonized waste cigarette filter adsorbent shows a profound potential as a sustainable solution to combat textile dye water pollution and cigarette filter pollution simultaneously, due to its low cost, simple preparation, and

versatility in application.

Keywords: doped carbon; adsorption; green chemistry, microwave, cigarette

1. Introduction

The textile industry contributes to a considerable amount of water pollution worldwide. According to the National Resources Defense Council, textile mills generate approximately 20% of industrial water pollution, during which an approximate 20,000 different chemicals contaminate water [1]. It is estimated that 500,000 textile dyes are produced yearly; these synthetic dyes are immensely stable to light, temperature, and chemical treatment. Moreover these synthetic dyes are resistant to biodegradation under aerobic conditions, and exhibit a high level of solubility in aqueous solutions with visibility to the naked eye at concentrations as low as 1 ppm [2]. Due to these characteristics, current large-scale effluent treatments are ineffective for dye removal and high in cost, resulting in an estimated 20% of dyes being released into the environment.

Several prominent chemical and physical methods are used currently for textile dye removal from effluents, such as coagulation-flocculation, aerobic degradation, and adsorption [3]. Adsorption is a common choice to remove dye from solution as it is a

47 relatively simple and inexpensive method [4,5]. Adsorbents researched for dye removal
48 include commercially-available and waste-generated activated carbon utilizing
49 precursors such as tea [6], chitosan [7], and citrus peels [8]. There are also an
50 increasing number of reports using heteroatoms such as nitrogen [9–11], phosphorus
51 [12], or sulfur [13] - doped activated carbon materials, to achieve enhanced
52 adsorption. Many materials have shown promising results using dual or co-doping with
53 two different elements [14,15]. In this work, CF waste will be explored as a carbon
54 precursor for synthesis of co-doped carbon material.

55 Cigarette waste contributes to the largest amount of plastic pollution around the
56 world [16]. Most cigarette filters (CFs), the part of the cigarette that remains after
57 smoking, are tossed onto the ground, leading to an immense ecological pollution. CFs
58 are composed mainly of plastic, viz. cellulose acetate, which is not readily
59 biodegradable [17]. Additionally, CFs contain toxic metals that can be leeched into soil
60 and water, causing direct harm to plants and animals [18]. Due to the posed ecological
61 threat of the litter, new methods of reducing cigarette pollution are needed. Since CFs
62 are comprised mostly of cellulose acetate, a carbon-based polymer, these waste
63 products can easily be utilized as carbon precursors for production of activated carbons

64 [19–21].

65 This work aims to convert used CF into useful carbon adsorbents via inexpensive
66 and facile microwave-assisted approach. The phosphorus and nitrogen heteroatom –
67 doped carbon contains functional groups which may have a synergistic effect on the
68 adsorption capacity. Both undoped and doped carbons from CF are characterized in
69 detail. Methylene blue (MB) dye is used to investigate the adsorption characteristics of
70 the newly developed phosphorus and nitrogen co-doped carbon from cigarette filter
71 (DCCF) and undoped carbonized cigarette filter (CCF). To the best of our knowledge,
72 no work has reported the use of this one-step microwave-assisted method for producing
73 DCCF and its use as an adsorbent.

74 2. Materials and methods

75 *2.1. Chemicals*

76 Waste CFs were collected from the University of Arkansas in Little Rock campus
77 and washed with deionized water to remove any dirt residue, and then they were dried
78 in air prior to their use. The paper casing was removed prior to carbonization.
79 Ammonium polyphosphate (APP, avg mw: 97) was a donation from JLS Chemicals.
80 ACS reagent grade sodium nitrate ($NaNO_3$) was purchased from ACROS. Methylene

blue (MB) dye was purchased from Sigma Aldrich. Triply deionized water (18.2 MΩ cm) was obtained using Elga model PURELAB ultra water-filtration system. Reagent grade hydrochloric acid (HCl) and sodium hydroxide (NaOH) were purchased from VWR and dilute 0.01 M solutions were used to adjust pH.

2.2. Adsorbent synthesis

Waste CFs were collected from receptacles located around UA Little Rock campus and carbonized through a facile, low-cost, microwave-assisted method described previously [22]. For DCCF synthesis, the CFs were weighed and combined with APP in a mass ratio of 1:0.4 g, and 2 drops of water was added to help initiate microwave carbonization process. An undoped carbonized sample of used CF (CCF) was prepared without APP. In this regard, CF with 2 drops of water were placed into a boron nitride crucible, which was promptly situated in a foamed aluminum oxide box to contain the reaction. The box was microwaved for 30 min at high power (2.45 GHz and 1.25 kW power) to carbonize the waste filters and then cooled to room temperature after which the resulting products were powdered using a mortar and pestle. This powder was placed in a container and stored in a desiccator for later use.

2.3. Physical characterization

Physical characterization of CF and DCCF were performed using several techniques. A JSM-7000F scanning electron microscope (SEM) was utilized to determine the morphology and percent elemental composition of the bulk materials. For SEM imaging, a small amount of sample was placed on a double-sided carbon tape on aluminum mount substrate before analysis. ASAP 2020 Micrometrics surface area and porosity analyzer with Brunauer–Emmett–Teller (BET) method was used to analyze surface area and pore size of materials via nitrogen adsorption/desorption studies at a bath temperature of 77 K. Thermo K-Alpha X-ray photoelectron spectrometer (XPS) system was used to determine surface elemental composition of dried carbonized samples. Fourier transform infrared (FTIR) spectroscopy was performed using a Thermo Scientific Nicolet 6700 Spectrometer to confirm that MB was adsorbed onto adsorbent surface and not degraded during adsorption. To determine point of zero charge (PZC), a simple salt addition method was used. Briefly, a suspension of adsorbent (0.01 g) was prepared in 0.1 M $NaNO_3$ aqueous solution in different reaction vessels (5 g L^{-1} CCF or DCCF).

2.4. Adsorption studies

2.4.1. Adsorbent dosage

To optimize the adsorbent dosage for adsorption, various masses (5-20 mg) were contacted with 50 mL of 10 ppm MB solution. After reaching equilibrium (24 h), the treated MB solutions were centrifuged at 3800 RPM for 10 min to separate the dye solution from the adsorbent. Absorption spectrophotometry (Lambda 850 UV-vis spectrophotometer with 1 cm path length quartz cuvette) was utilized to determine the concentration of MB remaining in solution at equilibrium. From this, the percent removal and adsorption capacity were determined.

2.4.2. Initial concentration

To analyze the effects of MB concentration on the adsorption onto CCF and DCCF from CFs, batch adsorption tests were performed. Using the MB stock solution, 50 mL MB solutions were prepared with varying concentration (5 ppm to 100 ppm). 10 mg samples of the carbon from the CF and a magnetic stir bar were placed into each of the MB solutions. The solutions were stirred at room temperature at constant speed until they reached equilibrium. The equilibrium data was then fitted into Langmuir and Freundlich isotherm models to determine how the MB interacts with CCF and DCCF.

2.4.3. Adsorption kinetics

To understand how the uptake of MB by CCF and DCCF is affected by time,

adsorption kinetic tests were performed. Samples containing 50 mL of various initial concentration of MB solution (5-100 ppm) were prepared and contacted with 10 mg of adsorbent powder and stirred using a magnetic stir bar after which a timer was immediately started. After specified time intervals, an aliquot of the MB solution was analyzed by absorbance spectroscopy. This data was fit into pseudo-first and second order equation to determine the primary mechanism of adsorption for the two materials.

2.4.4. Effect of temperature

Solutions of MB were prepared at 30 ppm and adjusted to various temperatures: 25, 35, 45, and 55 ^{o}C. Then, 10 mg of adsorbent was added and stirred for 24 h. Afterwards, remaining concentration of MB dye was analyzed via absorbance spectrophotometry and adsorption capacity was calculated.

2.4.5. Effect of pH

Test solutions were prepared using dilute concentrations of HCl and NaOH. 10 mg of adsorbent was contacted with 50 mL of 30 ppm initial concentration of MB solution in the flask. The mixture containing constant amount of adsorbent and constant concentration of MB dye was stirred at 120 rpm until equilibrium was achieved (24 h) at various initial pH.

3. Results and discussion

3.1. Physical characterization

3.1.1. SEM

Surface morphology of carbonized waste cigarette filters was determined by SEM imaging. SEM image of CCF exhibits a rigid amorphous structure with smaller microstructures decorated on the surface (Figure 1a). Images of DCCF sample display cave-like structures and ridges at the macrostructure with spherical microscale structures distributed throughout (Figure 1b). The doped sample also exhibit more sponge-like morphology indicating that it possesses a more well-developed pore structure than the undoped adsorbent. In order to confirm this, surface area analysis by BET was also performed.

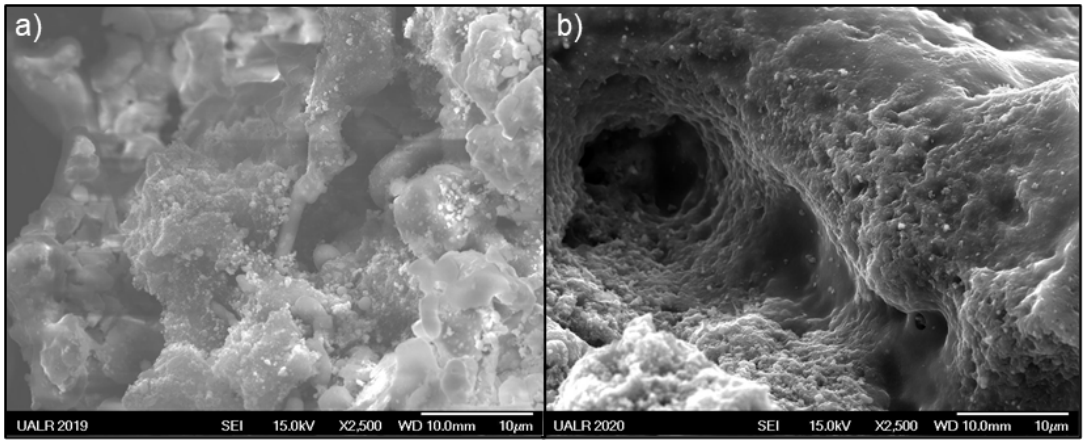

Figure 1. SEM images of a) CCF and b) DCCF adsorbents at 2,500 X magnification.

3.1.2. BET surface area analysis

Both adsorbents were characterized by BET in order to gain insight into their surface area and porosity. From adsorption-desorption isotherms, both adsorbents exhibit a type IV isotherm characterized by Langmuir-like behavior at relative low pressure and hysteresis loop at higher pressure (Figure 2) [23]. The hysteresis loop is formed by capillary condensation in the mesoporous structures of the material. The BET surface area of CCF and DCCF adsorbents are 176.5 and 177.6 $m^2 g^{-1}$, respectively. The microwave activation process causes the formation of reducing gases leading to high surface area carbon materials. This result indicates that doping with APP does not play a significant role in enhancing the overall surface area of the activated material. However, DCCF is significantly more mesoporous (87.6% mesopores by volume). This could be due to larger reducing gas formation when combined with APP. The overall results of BET analysis are tabulated in Table 1.

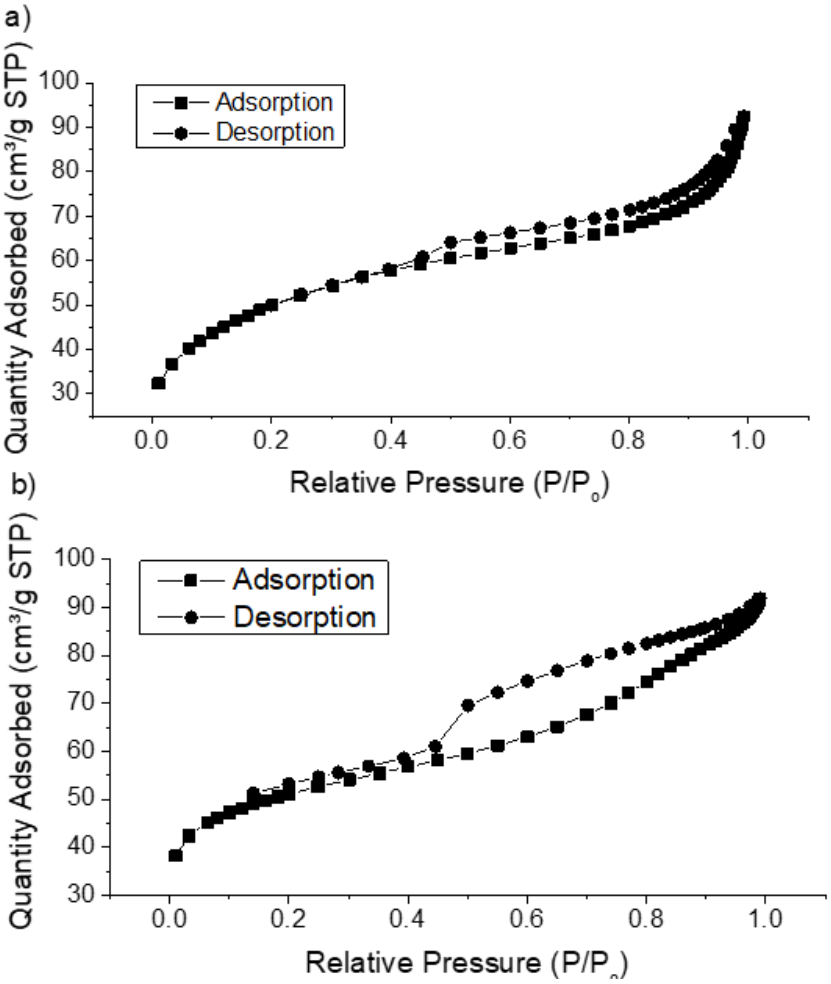

175

176 Figure 2. Adsorption and desorption curves of a) CCF and b) DCCF.

177 [Table 1]

178 3.1.3. XPS

179 In order to determine surface elemental composition of adsorbent materials, XPS

180 was performed. Various functional groups of atoms at the surface can greatly enhance

181 adsorption mechanism by allowing chemisorption processes to occur. Survey scan

182 spectra of both samples reveal the presence of carbon, oxygen, and phosphorus at the

183 surface (Figure 3). Results of CCF reveals the additional presence of silicon at a low

184 percentage (1.13%, Table 2). This is expected, as silicates can be formed in cigarette
185 smoke and deposited in the filter during smoking [24]. DCCF contains much greater
186 amount of phosphorus (3.98%) and nitrogen at the surface, confirming that the doping
187 of the material was successful. These elements at the surface of adsorbent can aid in
188 binding MB.

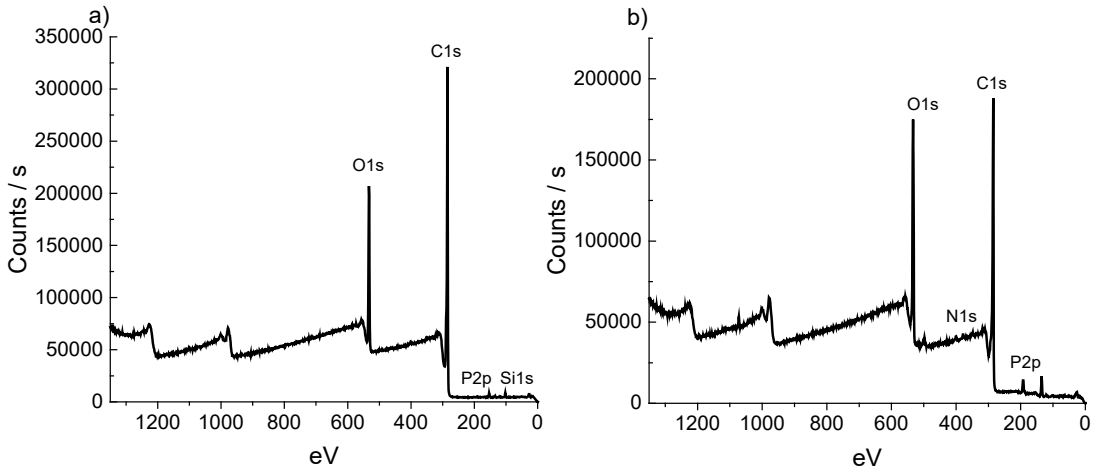

189

190 Figure 3. Survey scan plots of a) CCF and b) DCCF adsorbents

191 [Table 2]

192 3.1.4. PZC

193 The PZC of the adsorbents is analyzed in order to better understand the possible
194 adsorption mechanism onto the materials. The PZC can be defined as the pH where the
195 net charge of an adsorbent is zero. Since MB is a cationic dye, adsorption is favored
196 when the solution pH is greater than the PZC of an adsorbent (adsorbent carries net

197 negative charge). In order to determine PZC, a salt addition method was used as

198 described previously. A plot of ΔpH versus $pH_{initial}$ was formed where ΔpH=0 was

199 deemed to be the PZC (Figure 4). The PZC of CCF and DCCF were found to be 7.25

200 and 3.23, respectively. This implies that MB adsorption will be more favorable onto

201 the doped adsorbent (DCCF) at natural pH.

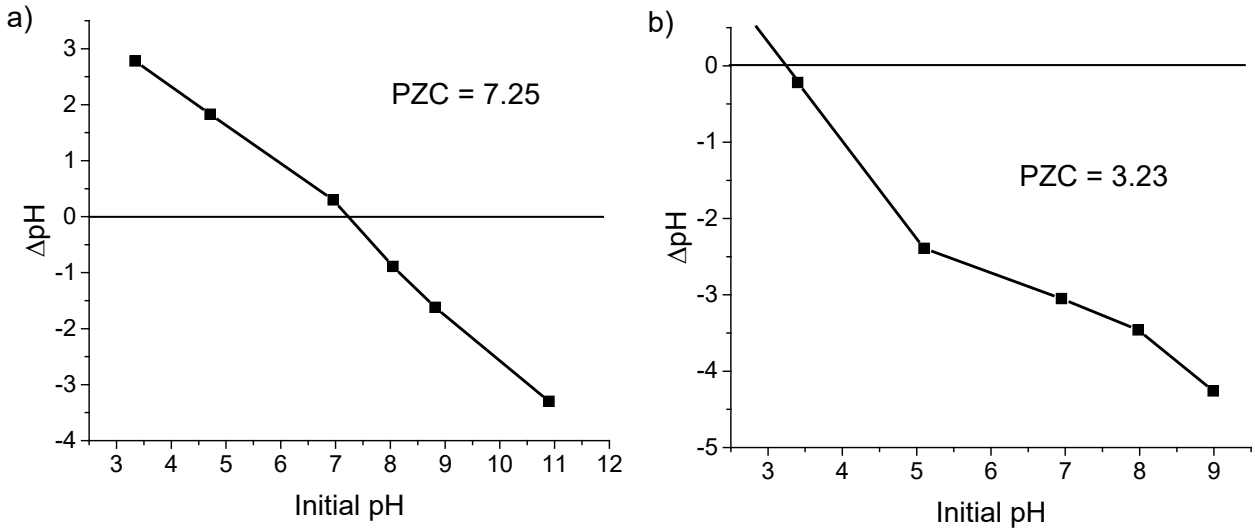

202

203 Figure 4. Point of Zero Charge (pH_{zc}) plots for a) CCF and DCCF.

204 3.1.5. FTIR

205 In order to confirm MB adsorption onto the doped adsorbent, FTIR was used to

206 identify characteristic carbon-sulfur bonds post-adsorption onto DCCF. Compared to

207 the raw adsorbent material, there are two additional peaks at 1191 and 1321 cm^{-1} which

208 are correlated to the C=S double bond and the C—S bond, respectively. The

introduction of these carbon sulfur bonds post-adsorption confirms that MB is adsorbed to the surface and is not degraded during adsorption process. A similar band at 1396 cm^{-1} was observed for CCF post MB adsorption (Figure S1), indicating a similar nondegradative adsorption process for the undoped sample as well.

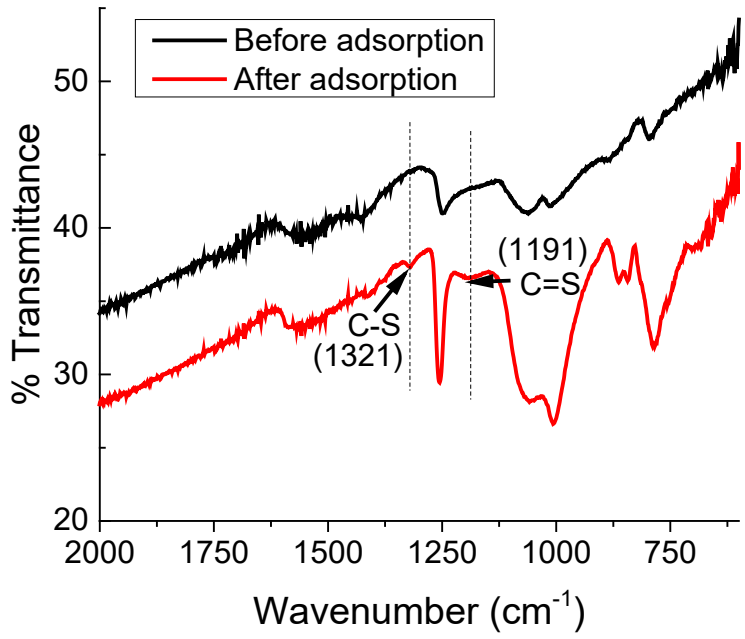

Figure 5. FTIR of DCCF adsorbent before and after adsorption of MB

3.2. Adsorption characterization

3.2.1. Adsorbent dosage:

Various masses of CCF or DCCF were contacted with 50 mL solutions of MB dye, separately, and allowed to reach equilibrium. Afterwards, the percent removal of dye was calculated using Equation 1.

$$Percent\ Removal = \left(\frac{C_0 - C_e}{C_0}\right) * 100 \quad (1)$$

Where C is the concentration of MB in solution initially and at equilibrium. The amount of dye adsorbed at equilibrium, Q_e (mg g^{-1}) was calculated by using the following Equation 2:

$$Q_e = \frac{(C_o - C_e)V}{W} \quad (2)$$

Where V is the volume of solution and W is the weight of adsorbent. For both samples, percent removal of dye increases with an increase in adsorbent dosage (Figure 6). However, Q_e increases to a maximum value and then decreases after a certain mass dosage. For CCF, the maximum Q_e value is obtained at a mass dosage of 10 mg. For DCCF, this occurs at a slightly lower mass of 7.5 mg. To keep conditions the same for both adsorbents, a mass loading of 10 mg is used for further adsorption experiments.

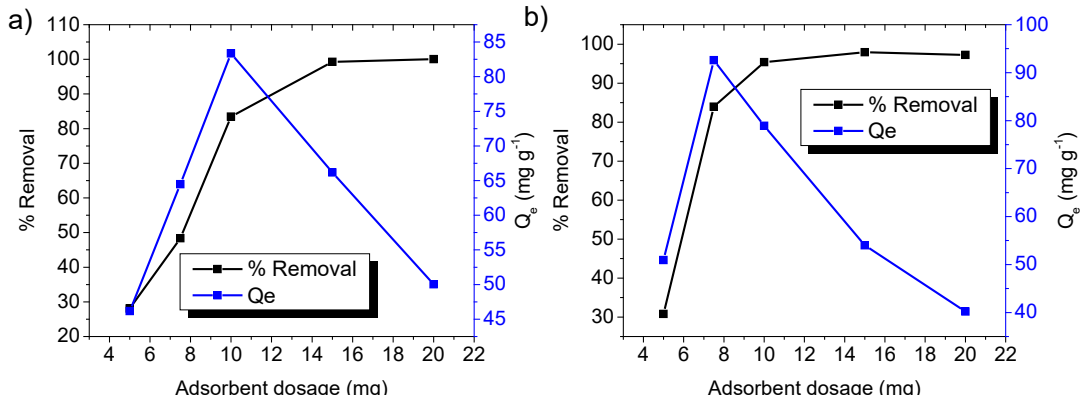

Figure 6. Effects of adsorbent dosage on adsorption capacities and % MB removal for a) CCF and b) DCCF.

3.2.2. Effect of initial concentration:

The effect of initial concentration of MB adsorption onto the adsorbents was investigated by contacting a fixed mass of 10 mg adsorbent to varying concentration of MB from 5-100 ppm. For both adsorbents, it was observed that the adsorption capacity increased as the initial concentration of MB increased (Figure 7). This is due to the mass transfer driving force between liquid-solid interface involved in heterogeneous adsorption. More dye molecules in the liquid phase shifts equilibrium toward adsorption onto the solid phase. Also, when the initial concentration is very low (5 ppm), both adsorbents exhibit a similar Q_e value. However, for CCF, the maximum Q_e value achieved is 194.6 mg g^{-1} while DCCF reaches a value of 293.45 mg g^{-1}. This indicates the enhanced adsorptive capabilities of DCCF compared to CCF.

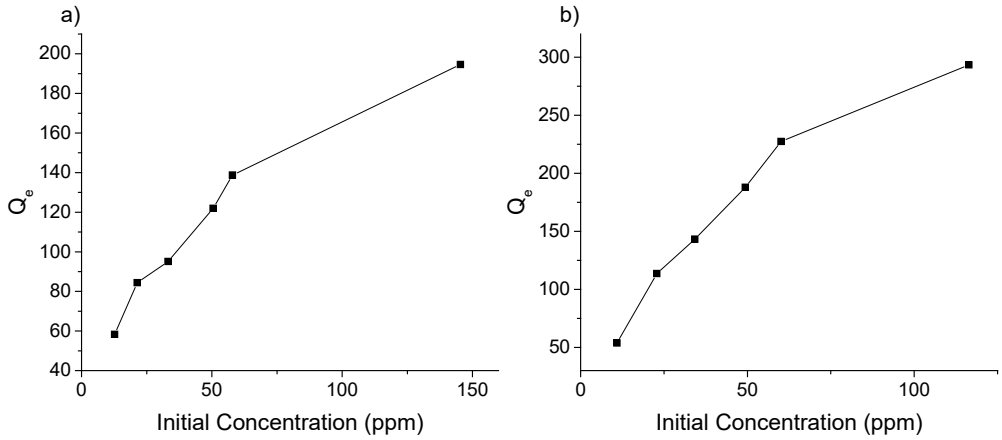

Figure 7. Effects of initial MB concentration on the equilibrium adsorption capacity of a) CCF and b) DCCF.

3.2.3. Adsorption isotherms:

Adsorption isothermal modelling of the data allows a detailed investigation of possible adsorption mechanisms. The models help to describe the interactions between adsorbent and dissolved dye species at the liquid-solid phase boundary and allow an estimation of the maximum adsorption capacity. The two most common models, Langmuir and Freundlich models, have been applied to the adsorption data of CCF and DCCF samples.

Modelling with the Langmuir equation is performed with several assumptions, one being that only a monolayer of adsorbate can be adsorbed onto the active sites of an adsorbents, and there is a limited amount of these sites. The model also makes the assumptions that those active sites are energetically equivalent regardless of their occupation, meaning the Langmuir equation does not consider repulsive forces of molecules bound to adsorbent surface. The linear form of the Langmuir equation [25] (Equation 3) was used to determine the Langmuir constants related to maximum adsorption amount per unit gram of adsorbent (Q_{max}) and related to the energy of adsorption (K_L)

$$\frac{C_e}{Q_e} = \frac{1}{Q_{max}K_L} + \frac{1}{Q_{max}}C_e \quad (3)$$

From the slope of Equation 3, Q_{max} can be obtained and was determined to be 212.8 and 303.0 mg $g^{-1}$for CCF and DCCF, respectively (Table 3). This indicates that DCCF possesses a higher capacity to adsorb MB from solution. The K_L value of DCCF is also much higher than CCF (0.38 vs 0.08) indicating a stronger interaction between doped sample surface and the adsorbate. Both models showed reasonable fitting with R^2 values of 0.911 and 0.986 for CCF and DCCF, respectively.

Modelling with the Freundlich equation is done with the assumptions that the adsorbent surface is heterogeneous and that the adsorption sites are of varying energy. The Freundlich equation (Equation 4) was also used in the linear form:

$$logQ_e = logK_F + \frac{1}{n} logC_e \quad (4)$$

Where K_F and n are constants related to adsorption capacity and intensity, respectively. Neither adsorbent was well represented by the model with R^2 values less than 0.88 in both cases. However, both adsorbents possess an n value greater than 1 which is indicative of a favorable process of adsorption. The n value of DCCF is greater than that of CCF (Table 3) which can be correlated to a stronger interaction between adsorbate and adsorption sites on the surface of the adsorbent material. K_F values are

281 related to adsorption capacity and, like Langmuir modelling of the data, DCCF exhibits
282 a higher K_F value. Langmuir and Freundlich fitting plots are displayed in Figure S2.
283 To investigate the spontaneity of the adsorption onto the two different adsorbents,
284 Gibbs free energy was calculated from Equation 5.
285 $$\Delta G^o = -RTlnk_0 \quad (5)$$
286 where R is the gas constant (8.314 J mol^{-1} K^{-1}) and T is the temperature (298 K), and
287 k_0, is equal to Q_e/C_e [26]. Both CCF and DCCF exhibited spontaneous adsorption
288 processes, indicated by negative values of ΔG^o. DCCF value of ΔG^o is lower than CCF,
289 indicating increased spontaneity of adsorption process upon conversion to doped
290 carbon material. ΔG^o values for both adsorbents are listed in Table 3.
291 [Table 3]
292 3.2.4. Kinetics
293 In order to gain insight on the kinetic mechanism of adsorbents, kinetic adsorption
294 was fitted into pseudo-first and pseudo-second order kinetic models. Experiments were
295 performed by varying initial concentration from 5 to 100 ppm of MB at natural pH and
296 recording the dye concentration at various time intervals after contact with adsorbent

297 (Figure 8a and 8b). The pseudo-first order model was used in the linear form (Equation
298 6) in order to evaluate the first order rate constant, k_1.

299 $$\log(Q_e - Q_t) = logQ_e - \frac{k_1}{2.303}t \quad (6)$$

300 Where Q_t is the amount of dye adsorbed at time, t. R^2 values were used to determine
301 the better fitting model. The pseudo-second order equation was also used in the linear
302 form (Equation 7) to determine second order rate constant, k_2.

303 $$\frac{t}{Q_t} = \frac{1}{k_2 Q_e^2} + \frac{1}{Q_e}\ \mathrm{t} \quad (7)$$

304 Plotting the linear form of Equation 6 and 7 generates a straight line in which k can
305 be directly calculated (Figure 8c, 8d, S2a, and S2b). CCF average R^2 value is 0.88
306 (Table S1) while the average value of R^2 for second order fitting is 0.99. This indicates
307 a better fitting of CCF adsorption to pseudo-second order kinetics. DCCF average R^2
308 value for pseudo-first order plot is 0.90 while for pseudo-second, the value average is
309 0.99. This indicates that the adsorption mechanism is better correlated to a pseudo-
310 second order process for both samples. This process is characterized by strong
311 chemisorptive adsorption between MB and CCF and DCCF adsorbents. In addition, the
312 standard deviation was calculated from Equation 8:

313 $$\Delta Q(\%) = 100 \times \sqrt{\frac{\sum[\frac{Q_{t,exp} - Q_{t,cal}}{Q_{t,exp}}]^2}{n-1}} \quad (8)$$

For CCF adsorption, ΔQ was found to be between 1.03-8.48 for second order compared to 6.98-19.90 for first order (Table S1). Similarly, DCCF displayed ΔQ values between 4.52-16.97 for pseudo-first order and 4.89-8.44 for pseudo-second order. This data further supports a chemisorptive mechanism of adsorption for the two adsorbents.

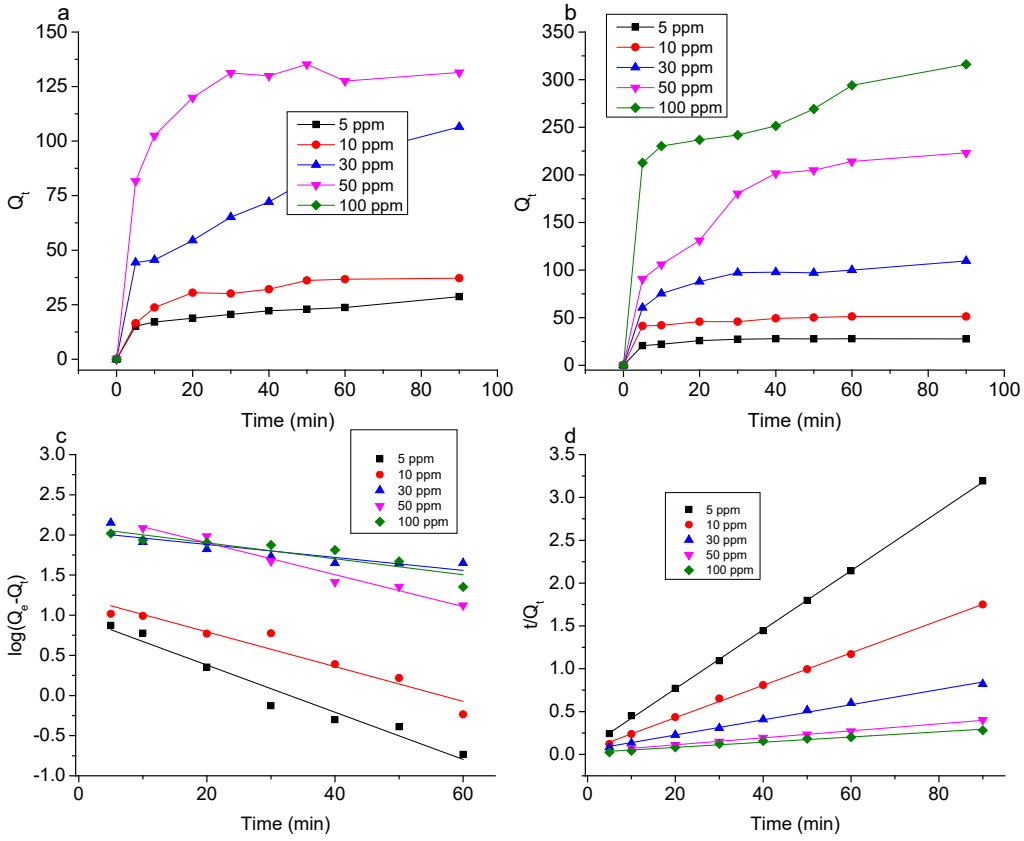

Figure 8. Kinetics plot of a) CCF and b) DCCF and pseudo c) first and d) second order fitting of data of doped sample.

The adsorption capacity of CCF and DCCF were compared to those of other waste-derived carbon materials for their removal of MB from solution. The waste precursors

and corresponding maximum adsorption capacities are reported in Table 4. From this data, it can be concluded that CCF and DCCF show exceptional application as adsorbent materials for removal of the cationic MB dye as their adsorption capacities are higher than many other waste-derived carbons. Additionally, many of the previously used waste precursors require chemical activation, whereas this work highlights a simplistic method to produce doped carbons with desirable adsorption characteristics.

[Table 4]

3.2.5. Effect of temperature:

In order to evaluate the temperature effect on adsorption onto the cigarette-based samples, experiments were performed at four different temperatures ranging from 25 to 55 ºC. It is observed that for both adsorbent materials, the adsorption capacity, Q_e is increasing as the temperature increases (**Figure 9**). This is due to an increased diffusion rate of MB molecules into the internal cavities of porous carbons [25]. This occurs mainly due to the lowering of viscosity of the solvent as temperature increases. This is also indicative of an endothermic adsorption process for both adsorbents [27].

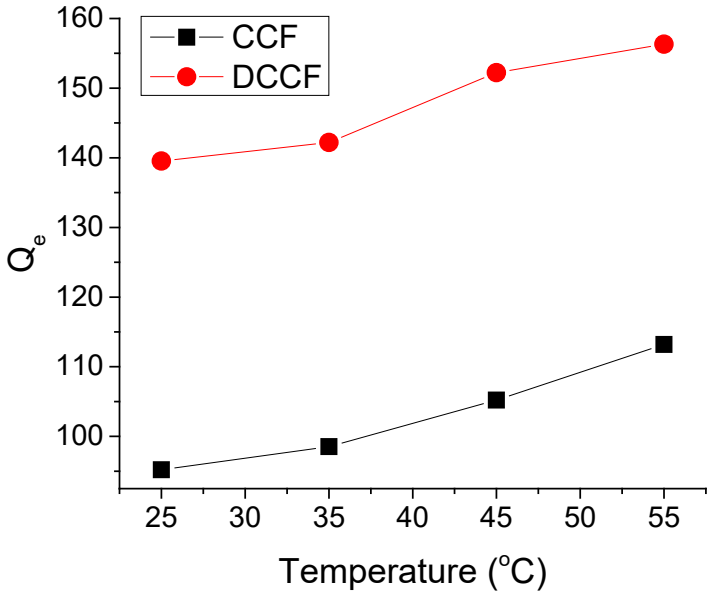

Figure 9. Effect of temperature on equilibrium adsorbent capacity from initial concentration of 30 ppm and 10 mg adsorbent dosage.

3.2.6. Effect of pH:

The effect of solution pH on MB adsorption was determined by contacting 10 mg of adsorbent to 50 mL of 30 ppm MB solution (**Figure 10**). CCF adsorption is greatly dependent on pH, ranging from 77.6 mg/g to 99.7 mg/g in a pH range from 3.9 to 10.2. This is due to the neutral PZC of CCF. Below pH 7, the adsorption is unfavored because of the repulsive forces between MB and the positive adsorbent surface. In contrast, DCCF adsorption capacity remains relatively unchanged over the pH range 3.35 to 10.89. This is because of a low PZC value of DCCF, causing it to have a net negative surface charge at pH past 3.23.

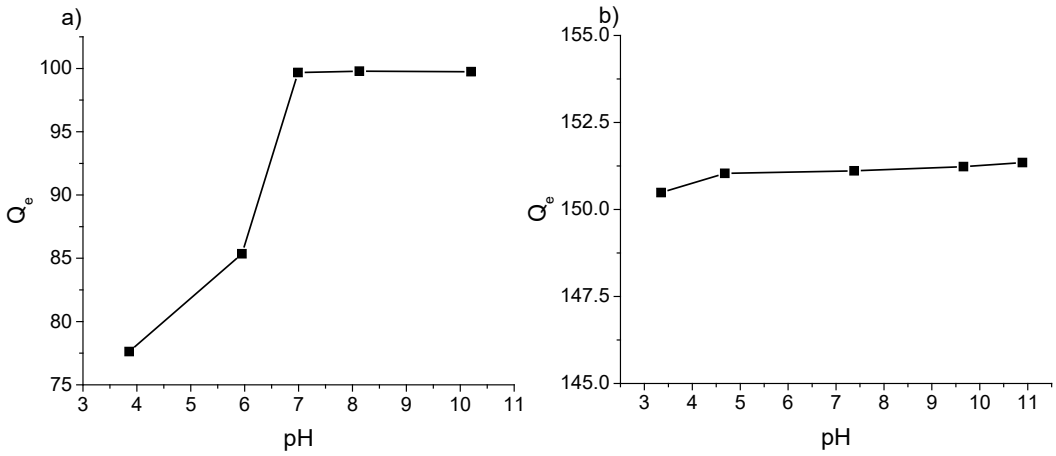

Figure 10. Effect of initial solution pH on adsorption capacity of a) CCF and b) DCCF using an initial 50 mL of 30 ppm MB solution.

4. Conclusions

Useful adsorbent materials were successfully prepared from waste CCF using a simple and rapid one-step microwave synthesis. DCCF exhibited an exceptional maximum adsorption value of 303.0 mg g^{-1}, making it a very efficient and low-cost adsorbent. The materials were characterized in detail to reveal crucial information about their surface area, elemental composition, and morphology. The adsorbents were found to have high surface area (~177 m^2 g^{-1}) and well-developed porosity. Doping of the sample was confirmed using XPS which showed significant contribution of phosphorus and nitrogen on the surface of the material which played a significant role in enhancing the adsorption capacity of the material. Adsorption of MB onto adsorbents was found to be best correlated to a monolayer adsorption process as confirmed by higher R^2 value with Langmuir fitting. Further, the adsorbents undergo a pseudo-

second order adsorption process which is indicative of a chemisorptive process. Adsorption onto the adsorbents is spontaneous ($\Delta G<0$) and endothermic in nature. This work highlights an inexpensive and green method to convert a common litter source into a useful material for water remediation.

Declarations

Availability of data and materials

The datasets generated during and/or analyzed during the current study are available from the corresponding author on reasonable request**.**

Competing interests

The authors declare they have no competing interests.

Funding

This research acknowledges the Signature award funding and startup funds from the University of Arkansas at Little Rock

Authors' contributions

S.M., Z.A, A.I., and S.A collected adsorption data and performed data analysis. S.M. and F.W. collected physical characterization data. T.V. and N.S. provided supervision, project administration, and acquisition of funding. Writing and original

draft preparation was conducted by S.M. and N.S. All authors read and approved the final manuscript.

Acknowledgements

The authors acknowledge Center for Integrative Nanotechnology Sciences for characterization instrumentation.

References

1. Greer B, Maul R, Campbell K, Elliott CT. Detection of freshwater cyanotoxins and measurement of masked microcystins in tilapia from Southeast Asian aquaculture farms. Anal Bioanal Chem 2017;409:4057–69.
2. Lellis B, Fávaro-Polonio CZ, Pamphile JA, Polonio JC. Effects of textile dyes on health and the environment and bioremediation potential of living organisms. Biotechnol Res Innov 2019;3:275–90.
3. Mazille F, Spuhler D. Coagulation-Flocculation. 2014.
4. Kandisa RV, Saibaba KV N. Dye Removal by Adsorption: A Review. J Bioremediation Biodegrad 2016;07.
5. Buhani, Wijayanti TA, Suharso, Sumadi, Ansori M. Application of modified green algae Nannochloropsis sp. as adsorbent in the simultaneous adsorption of

Methylene Blue and Cu(II) cations in solution. Sustain Environ Res 2021;31:1–12.

6. Sikdar D, Goswami S, Das P. Activated carbonaceous materials from tea waste and its removal capacity of indigo carmine present in solution: synthesis, batch and optimization study. Sustain Environ Res 2020;30:1–16.

7. Liang B, Li K, Liu Y, Kang X. Nitrogen and phosphorus dual-doped carbon derived from chitosan: An excellent cathode catalyst in microbial fuel cell. Chem Eng J 2019;358:1002–11.

8. Nageeb M. Adsorption Technique for the Removal of Organic Pollutants from Water and Wastewater. Org. Pollut. - Monit. Risk Treat., InTech; 2013.

9. Li H, An N, Liu G, Li J, Liu N, Jia M, et al. Adsorption behaviors of methyl orange dye on nitrogen-doped mesoporous carbon materials. J Colloid Interface Sci 2016;466:343–51.

10. Lian F, Cui G, Liu Z, Duo L, Zhang G, Xing B. One-step synthesis of a novel N-doped microporous biochar derived from crop straws with high dye adsorption capacity. J Environ Manage 2016;176:61–8.

11. Wang Z, Wang K, Wang Y, Wang S, Chen Z, Chen J, et al. Large-scale fabrication

of N-doped porous carbon nanosheets for dye adsorption and supercapacitor applications. Nanoscale 2019;11:8785–97.

12. Silva TL, Cazetta AL, Souza PSC, Zhang T, Asefa T, Almeida VC. Mesoporous activated carbon fibers synthesized from denim fabric waste: Efficient adsorbents for removal of textile dye from aqueous solutions. J Clean Prod 2018;171:482–90.

13. Vigneshwaran S, Sirajudheen P, Karthikeyan P, Meenakshi S. Fabrication of sulfur-doped biochar derived from tapioca peel waste with superior adsorption performance for the removal of Malachite green and Rhodamine B dyes. Surfaces and Interfaces 2021;23:100920.

14. Macchi S, Siraj N, Viswanathan T. Kinetic and mechanistic study of dye sorption onto renewable resource-based doped carbon prepared by a microwave-assisted method. Environ Technol 2020.

15. Roldán L, Marco Y, García-Bordejé E. Bio-sourced mesoporous carbon doped with heteroatoms (N,S) synthesised using one-step hydrothermal process for water remediation. Microporous Mesoporous Mater 2016;222:55–62.

16. Qamar W, Abdelgalil AA, Aljarboa S, Alhuzani M, Altamimi MA. Cigarette

waste: Assessment of hazard to the environment and health in Riyadh city. Saudi J Biol Sci 2020;27:1380–3.

17. Puls J, Wilson SA, Hölter D. Degradation of Cellulose Acetate-Based Materials: A Review. J Polym Environ 2011;19:152–65.

18. Moerman JW, Potts GE. Analysis of metals leached from smoked cigarette litter. Tob Control 2011;20:30–5.

19. Xiong Q, Bai Q, Li C, Li D, Miao X, Shen Y, et al. Nitrogen-doped hierarchical porous carbons from used cigarette filters for supercapacitors. J Taiwan Inst Chem Eng 2019;95:315–23.

20. Lee M, Kim GP, Don Song H, Park S, Yi J. Preparation of energy storage material derived from a used cigarette filter for a supercapacitor electrode. Nanotechnology 2014;25:345601.

21. Kim GP, Lee M, Song HD, Bae S, Yi J. Highly efficient supporting material derived from used cigarette filter for oxygen reduction reaction. Catal Commun 2016;78:1–6.

22. Macchi S, Siraj N, Watanabe F, Viswanathan T. Renewable-Resource-Based Waste Materials for Supercapacitor Application. ChemistrySelect 2019;4:492–

501.

23. Sing KSW, Everett DH, Haul RAW, Moscou L, Pierotti RS, Rouquerol J, et al. Reporting physisorption data for gas/solid systems with special reference to the determination of surface area and porosity. Pure Appl Chem 1985;57:603–19.

24. Pappas RS. Toxic elements in tobacco and in cigarette smoke: Inflammation and sensitization. Metallomics 2011;3:1181–98.

25. Nasuha N, Hameed BH, Din ATM. Rejected tea as a potential low-cost adsorbent for the removal of methylene blue. J Hazard Mater 2010;175:126–32.

26. Archin S, Sharifi SH, Asadpour G. Optimization and modeling of simultaneous ultrasound-assisted adsorption of binary dyes using activated carbon from tobacco residues: Response surface methodology. J Clean Prod 2019;239.

27. Li Z, Hanafy H, Zhang L, Sellaoui L, Schadeck Netto M, Oliveira MLS, et al. Adsorption of congo red and methylene blue dyes on an ashitaba waste and a walnut shell-based activated carbon from aqueous solutions: Experiments, characterization and physical interpretations. Chem Eng J 2020;388:124263.

28. Danish M, Ahmad T, Majeed S, Ahmad M, Ziyang L, Pin Z, et al. Use of banana trunk waste as activated carbon in scavenging methylene blue dye: Kinetic,

thermodynamic, and isotherm studies. Bioresour Technol Reports 2018;3:127–37.

29. Reffas A, Bernardet V, David B, Reinert L, Lehocine MB, Dubois M, et al. Carbons prepared from coffee grounds by H3PO4 activation: Characterization and adsorption of methylene blue and Nylosan Red N-2RBL. J Hazard Mater 2010;175:779–88.

30. Rashid RA, Jawad AH, Ishak MABM, Kasim NN. FeCl3-activated carbon developed from coconut leaves: Characterization and application for methylene blue removal. Sains Malaysiana 2018;47:603–10.

31. Hu W, Xie Y, Lu S, Li P, Xie T, Zhang Y, et al. One-step synthesis of nitrogen-doped sludge carbon as a bifunctional material for the adsorption and catalytic oxidation of organic pollutants. Sci Total Environ 2019;680:51–60.

32. Dorothy A, Mideen AS. Adsorption of Methylene blue dye on activated carbon from rice husk. J Chem Pharm Res 2015;7:761–5.

33. Jasper EE, Ajibola VO, Onwuka JC. Nonlinear regression analysis of the sorption of crystal violet and methylene blue from aqueous solutions onto an agro-waste derived activated carbon. Appl Water Sci 2020;10:132.

485 **Table 1**. Surface area characteristics from BET.

Sample	BET surface area ($m^2 g^{-1}$)	Pore volume ($cm^3 g^{-1}$)	Micropore volume ($cm^3 g^{-1}$)	Mesopore volume ($cm^3 g^{-1}$)	Average pore width (Å)
CCF	176.5	0.140	0.042	0.098	31.7
DCCF	177.6	0.137	0.017	0.120	31.1

486 **Table 2.** Surface elemental composition (At%) of adsorbents

Element	CCF	DCCF
C1s	80.77	72.56
O1s	17.8	21.91
P2p	0.30	3.98
N1s	---	0.90
Si2p	1.13	---

487

488

489

490

491 **Table 3.** Langmuir and Freundlich constant value results from linear fitting and free

492 energy values for CCF and DCCF

Isotherm	Parameter	CCF	DCCF
Langmuir	Q_{max} (mg g^{-1})	212.8	303.0
	K_L (L mg^{-1})	0.08	0.38
	R^2	0.911	0.986
Freundlich	K_F (mg g^{-1}(L mg^{-1})1 n^{-1})	54.2	121.3
	n	3.85	4.55
	R^2	0.874	0.828
Gibb's free energy	ΔG^o (kJ mol^{-1})	-5.78	-11.1

493

494

495

496

497

498

499 **Table 4.** Comparison of maximum adsorption capacity of MB of CCF and DCCF to

500 other adsorbent materials (at 298 K).

Adsorbent precursor	Maximum capacity (mg g^{-1})	Reference
Carbonized cigarette filter (CCF)	212.8	This work
P and N co-doped cigarette filter (DCCF)	303.0	This work
Banana peel	227.2	[28]
Coffee grounds	181.8	[29]
Coconut leaves	66.0	[30]
Sludge	46.7	[31]
Rice husk	33.9	[32]
Seed pod	14.8	[33]

501

Supporting Information

Phosphorus and nitrogen co-doped carbon derived from Cigarette Filter for adsorption of methylene blue dye from aqueous solution

Samantha Macchi[1], Zane Alsebai[2], Fumiya Watanabe[3], Arooba Ilyas[1], Shiraz Atif[1], Tito Viswanathan[1] and Noureen Siraj[1,*]

[1] Department of Chemistry, University of Arkansas at Little Rock, 2801 S. University Ave, Little Rock, AR 72204, USA; spmacchi@ualr.edu, ZA, AI, SA, txviswanatha@ualr.edu, nxsiraj@ualr.edu

[2] Little Rock Central High School, 1500 Park Street, Little Rock, AR 72202, USA; zane.abdeen.alsebai@gmail.com

[3] Center for Integrative Nanotechnology Sciences, University of Arkansas at Little Rock, 2801 S. University Ave, Little Rock, AR 72204, USA; fxwatanabe@ualr.edu

* Correspondence: nxsiraj@ualr.edu; (501-916-6544)

FTIR

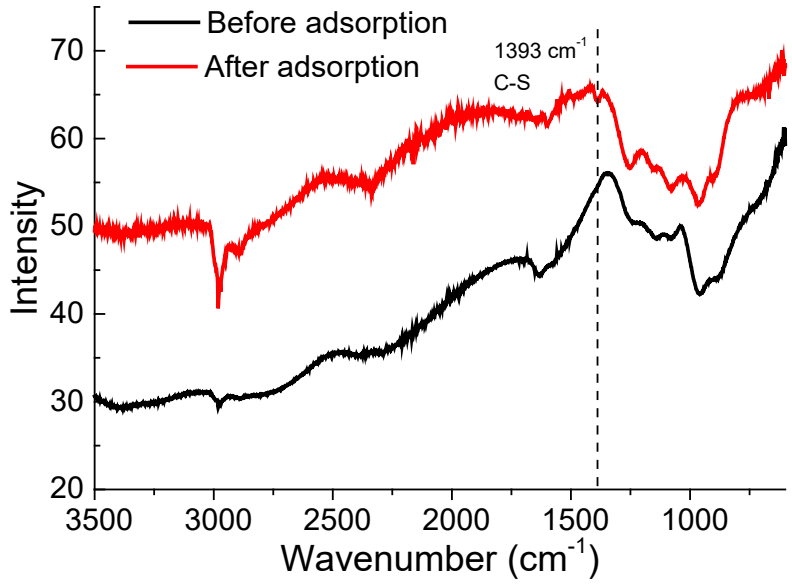

Figure S1. FTIR of CCF before and after adsorption

Adsorption modelling

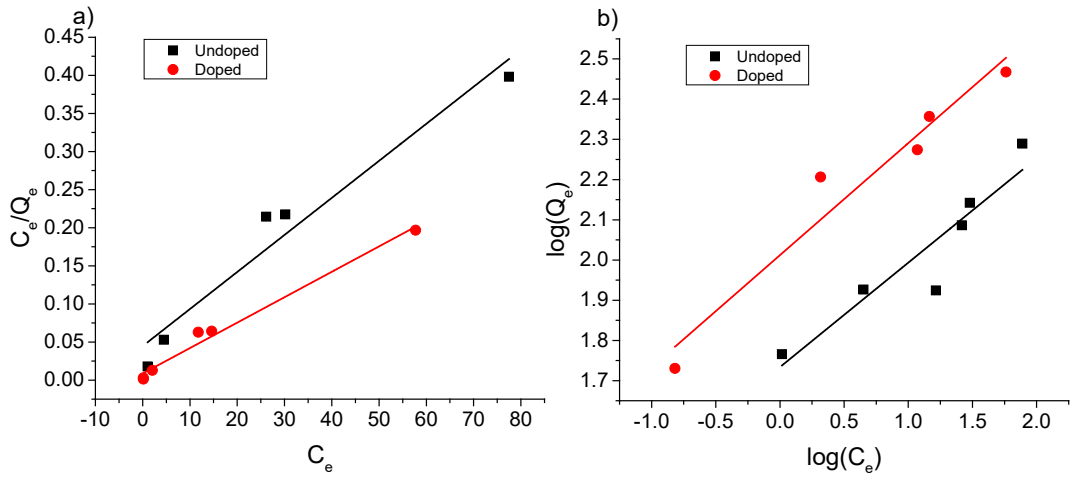

Figure S2. a) Langmuir fitting and b) Freundlich fitting of CCF and DCCF adsorption data from Figure 7.

Kinetic modelling of undoped sample data

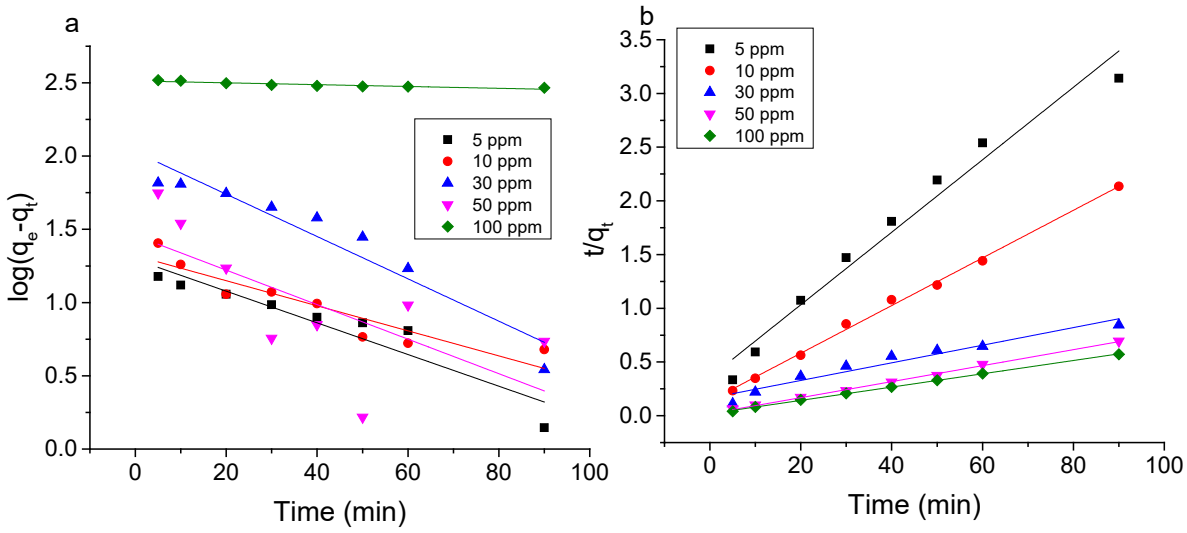

Figure S3. A) Pseudo first and b) pseudo second order fitting for CCF kinetic data from Figure 8a.

Table S1. Results of fitting of pseudo first and second order kinetic models on adsorption onto CCF and PNCF.

CCF									
Pseudo-first order					Pseudo-second order				
C_0 (ppm)	$Q_{e,cal}$ (mg/g)	k_1 (1/min)	R^2	Δq	C_0 (ppm)	$Q_{e,cal}$ (mg/g)	k_2 (g/mg · min)	R^2	Δq
5	26.15	0.00290	0.988	6.98	5	23.78	0.00661	0.995	8.05
10	44.67	0.00503	0.934	15.14	10	42.29	0.00326	0.993	1.03
30	99.71	0.00438	0.940	19.90	30	90.47	0.00097	0.978	8.48
50	134.24	0.00855	0.619	14.57	50	132.48	0.00193	0.995	5.90
100	176.42	0.00039	0.911	8.80	100	154.29	0.00030	0.999	6.78
DCCF									
Pseudo-first order					Pseudo-second order				
C_0 (ppm)	$Q_{e,cal}$ (mg/g)	k_1 (1/min)	R^2	Δq	C_0 (ppm)	$Q_{e,cal}$ (mg/g)	k_2 (g/mg · min)	R^2	Δq
5	28.47	0.00986	0.877	8.88	5	28.47	0.01479	0.999	6.79
10	51.92	0.00812	0.953	4.52	10	50.63	0.00740	0.998	4.89
30	100.84	0.00708	0.873	13.82	30	100.38	0.00578	1.000	5.36
50	222.93	0.00968	0.987	16.97	50	223.71	0.00039	0.989	7.93
100	300.40	0.00434	0.828	9.51	100	263.54	0.00117	0.995	8.44